

1
2
3 **Supraglacial river forcing of subglacial water storage and diurnal ice**
4 **sheet motion**
5
6

7 L.C. Smith^{1,2,3}, L.C. Andrews⁴, L.H Pitcher^{5,3}, B.T. Overstreet⁶, Å.K. Rennermalm⁷, M.G.
8 Cooper^{3,8}, S.W. Cooley^{9,3}, J.C. Ryan¹, C. Miège^{7,10}, C. Kershner^{11,13}, C.E. Simpson^{12,3}

9
10 ¹Institute at Brown for Environment and Society (IBES), Brown University, Providence, Rhode
11 Island, 02912, USA

12 ²Department of Earth, Environmental, and Planetary Sciences, Brown University, Providence,
13 Rhode Island, 02912, USA

14 ³Department of Geography, University of California - Los Angeles, Los Angeles, California,
15 90095, USA

16 ⁴ Global Modeling and Assimilation Office, NASA Goddard Space Flight Center, Greenbelt,
17 Maryland, 20771, USA

18 ⁵Cooperative Institute for Research in Environmental Sciences (CIRES), University of Colorado
19 – Boulder, Boulder, Colorado, 80303, USA

20 ⁶Department of Geology and Geophysics, University of Wyoming, Laramie, WY, 82071, USA

21 ⁷Department of Geography, Rutgers, The State University of New Jersey, New Brunswick,
22 08901, New Jersey

23 ⁸Atmospheric Sciences and Global Change Division, Pacific Northwest National Laboratory,
24 Richland, Washington, 99352, USA

25 ⁹Department of Earth System Science, Stanford University, Stanford, CA, 94305 Affiliation for
26 author 9.

27 ¹⁰Department of Geography, University of Utah, Salt Lake City, Utah, 84112, USA

28 ¹¹Research Directorate, National Geospatial-Intelligence Agency, Springfield, VA 22150

29 ¹²RedCastle Resources, Inc., Salt Lake City, Utah, 84138, USA

30 ¹³Department of Geography and Geoinformation Science, George Mason University, Fairfax,
31 VA 22030

32
33
34 Corresponding author: first and last name (laurence_smith@brown.edu)

35 **Key Points:**

- 36 • We present coincident field measurements of supraglacial river discharge and GPS-
37 derived ice motion on the southwest Greenland Ice Sheet ablation zone
- 38 • The measurements are obtained upstream of a major moulin, enabling study of how
39 supraglacial meltwater runoff influences subglacial hydrology and ice motion
- 40 • Recorded ice velocities are strongly correlated with measurements of supraglacial river
41 discharge acquired hourly over the 7-day study period
- 42 • Differencing of supra- and proglacial discharge hydrographs suggests that diurnal
43 fluctuations in subglacial water storage drive short-term variations in ice motion

44

45 **Abstract (150 words max)**

46 Surface melting can alter ice sheet sliding by supplying water to the bed, but subglacial processes
47 driving ice accelerations are complex. We examine linkages between surface runoff, transient
48 subglacial water storage, and short-term ice motion from 168 consecutive hourly measurements
49 of meltwater discharge (i.e. moulin input) and GPS-derived ice surface motion for Rio Behar, a
50 ~60 km² moulin-terminating supraglacial river catchment the southwest Greenland ablation
51 zone. Short-term accelerations in ice speed correlate strongly with lag-corrected measures of
52 surface mass loss, specifically supraglacial river discharge ($r=0.9$; $p<0.001$). Though our 7-day
53 record cannot address seasonal-scale forcing, diurnal ice accelerations align with normalized
54 differenced supraglacial and proglacial discharge, a proxy for subglacial storage change, better
55 than GPS-derived ice surface uplift. These observations counter theoretical steady-state basal
56 sliding laws and suggest that moulin- and proglacially induced fluctuations in subglacial water
57 storage, rather than absolute subglacial water storage, drive short-term ice accelerations.

58

59 **Plain Language Summary**

60 The importance of surface melting to Greenland ice sheet subglacial hydrology and ice sliding
61 dynamics is widely recognized but poorly constrained by field observations. We present 168
62 consecutive hours of rare in-situ meltwater runoff measurements from a large supraglacial river
63 draining the ice sheet surface, just upstream of its plummet into a major moulin. GPS
64 measurements of ice surface motion record brief accelerations in ice sliding speed that follow
65 daily cycles in meltwater entering the moulin. By comparing these measurements with
66 proglacial river discharges leaving the ice sheet, we identify daily fluctuations in subglacial
67 water storage that align with short-term accelerations in ice motion. These findings affirm the
68 importance of supraglacial rivers to subglacial water pressure and ice dynamics, even in
69 relatively thick ice >40 km inland from the ice terminus.

70

71

72

73

74 **1. Introduction**

75 Accurate models of ice-sheet response to climate change require good physical
76 understanding of interactions between surface melting, subglacial hydrology, and ice dynamics
77 (e.g., *Bell, 2008; Chu, 2014; Davison et al., 2019*). On the Greenland Ice Sheet (GrIS) ablation
78 zone, surface melting activates a perennial hydrologic system of supraglacial streams, rivers, and
79 lakes (*Irvine-Fynn et al., 2011; Rennermalm et al., 2013a; Lampkin and VanderBerg, 2014;*
80 *Pitcher and Smith, 2019*), which commonly drain into moulins forming a dynamic subglacial
81 drainage system that modifies basal pressures and ice motion (e.g. *Meierbachtol et al., 2013;*
82 *Van de Wal et al., 2008; Zwally et al., 2002; Bartholomew et al., 2012*). While early concerns
83 about warming-induced runaway sliding now seem unfounded (e.g. *Tedstone, et al., 2013;*
84 *2015; van de Wal et al., 2015; Flowers, 2018*), physical processes governing the link between
85 GrIS supraglacial meltwater runoff, ice sheet basal pressures, and ice sliding remain under
86 intense study (*Davison et al., 2019; Nienow et al., 2017; Williams et al. 2020*).

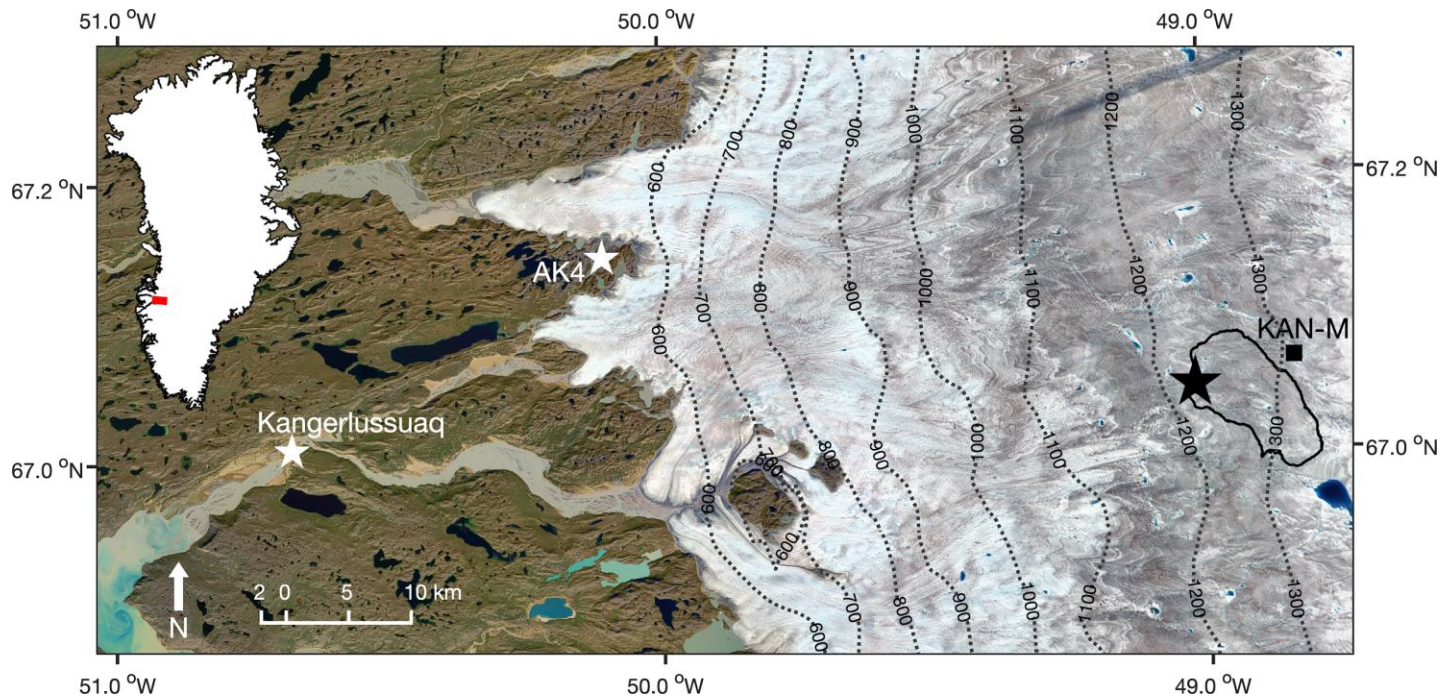
87 Traditional basal sliding law formulations linking subglacial pressure and ice motion
88 assume steady-state cavities at the bed (e.g. *Bindschadler, 1983; Schoof, 2005; Gagliardini et*
89 *al., 2007*). However, observational research suggests that subglacial cavities constantly undergo
90 transient evolution in response to fluctuations in supraglacial meltwater supply and subglacial
91 channelization (*Iken et al., 1983; Bartholomew et al., 2008; Hoffman et al., 2011; Cowton et al.,*
92 *2016; Andrews et al., 2018*). If so, highest subglacial water pressures (and therefore ice sliding
93 speed) should occur when transient cavities are growing fastest, not when they are largest (*Iken*
94 *et al., 1983; Cowton et al., 2016*).

95 Evidence for transient cavity evolution is drawn primarily from GPS-derived correlations
96 of horizontal ice speed with vertical ice surface uplift (interpreted as a proxy for total subglacial
97 water storage, S) or its first derivative (interpreted as subglacial water storage rate-of-change,
98 ΔS). GrIS horizontal ice sliding speed broadly covaries with vertical surface uplift over the time
99 scale of a melt season (e.g., *Hoffman et al., 2011; Bartholomew et al., 2010; Bartholomew et al.,*
100 *2012*), but variations at shorter timescales tend to correlate better with its derivative (*Hoffman et*
101 *al., 2011; Cowton et al., 2016; Andrews et al., 2018*). Such correlations are typically weak and
102 spatially variable due to a range of confounding factors impeding calculation of basal uplift from
103 ice surface elevation measurements (see *Andrews et al., 2018* and *Hoffman et al., 2011*).
104 Therefore, it is difficult to infer interactions between surface melting, subglacial water storage,
105 cavity growth, and ice motion for the GrIS, despite previous success on alpine glaciers (e.g.
106 *Bartholomew et al., 2008; 2011*).

107 To study the links among supraglacial runoff, subglacial water storage fluctuations, and
108 short-term ice motion, we present in situ measurements of moulin input (i.e. supraglacial
109 discharge), ice surface speed, and ice surface uplift for Rio Behar, a large supraglacial river on
110 the GrIS mid-elevation (>1200 m a.s.l.) ablation zone (**Figure 1**). We compare daily cycles in
111 these variables with PROMICE automated weather station measurements of surface energy
112 balance and ablation (*Fausto and van As, 2019*), and with proglacial discharges from permanent
113 river gauging stations located downstream (*Rennermalm et al., 2013b; 2017; van As et al., 2018;*
114 *2019*). Horizontal GPS positions provide ice surface speed variations, and vertical GPS
115 positions and their first derivative provide proxies for subglacial storage S and rate-of-change
116 ΔS , respectively. We also compute alternate, qualitative proxies for S and ΔS by differencing
117 normalized supraglacial and proglacial discharge hydrographs (adapted from *Bartholomew et*
118 *al., 2008, 2011* and *McGrath et al., 2011*). We conclude that diurnal cycles in moulin input

119 influence local ice speed variations through their influence on ΔS , confirming that transient water
 120 storage and cavity growth are important drivers of subglacial basal pressure and short-term ice
 121 motion.

122



123

124

125 **Figure 1: Study area in southwest Greenland. Black star shows location of our GPS measurements of ice surface**
 126 **motion and Acoustic Doppler Current Profiler (ADCP) measurements of moulin input (supraglacial discharge) in**
 127 **Rio Behar, a large supraglacial river penetrating the ice sheet >40 km from the ice edge. Measurements were**
 128 **acquired ~750 m upstream of the Rio Behar terminal moulin from 5-14 July 2017. Black outline denotes the Rio**
 129 **Behar surface catchment (60.02 km² in July 2016). White stars show locations of the PROMICE KAN_M**
 130 **automated weather station (black square) and two permanent gauging stations in proglacial rivers. Background**
 131 **is a 26 July 2016 true-color Landsat-8 satellite image.**

132

133 **2. Data and Methods**134 **2.1 Observational data**

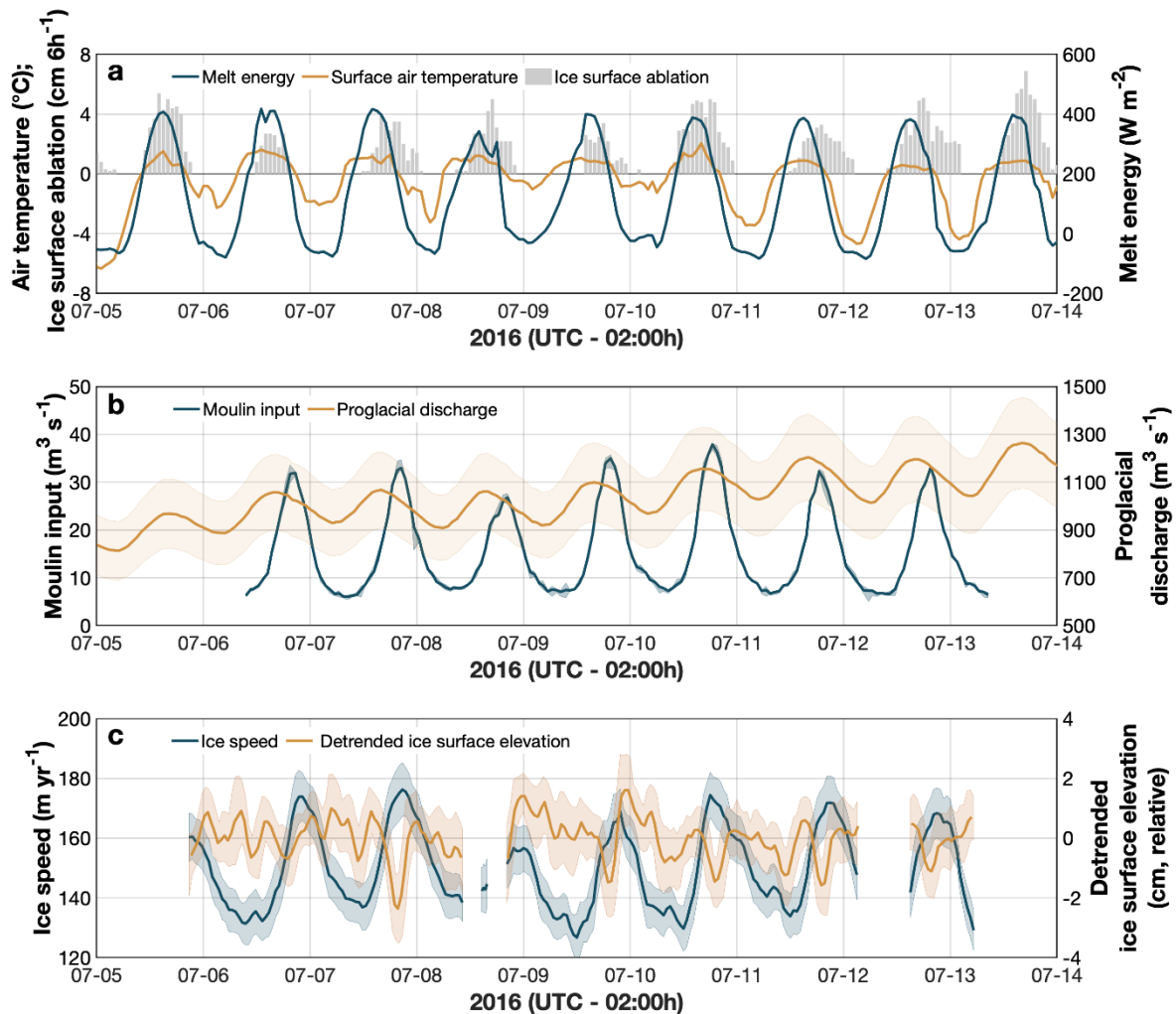
135 In July 2016 the Rio Behar terminal moulin was located at 67.047°N, -49.033°W, with an
 136 upstream drainage catchment of ~60.2 km² and mean surface elevation >1200 m (**Figure 1**). We
 137 established a field camp to monitor moulin meltwater input ~750 m upstream (location
 138 ~67.0499°N, -49.0180°W) and ice surface motion. Field operations were carried out from 5-14
 139 July 2016, with 168 consecutive hourly measurements of supraglacial river discharge collected
 140 6-13 July using a SonTek RiverSurveyor M9 Acoustic Doppler Current Profiler (ADCP) and
 141 methods of *Smith et al. (2017)*. A Tyrolean cableway was suspended over the river to safely and
 142 repeatedly tow the ADCP back and forth across the channel (**Figures S1-S4**). A total of 847
 143 ADCP transects were acquired, of which 677 later passed rigorous quality-assurance screening
 144 and were used to compute 174 hourly in situ discharge measurements (**Figure S5, Tables S1-S2,**
 145 **Datasets S1-S3**).

146 Simultaneous measurements of ice surface motion were collected every 5 seconds using a
 147 Trimble R7 GPS receiver and Trimble Zephyr Geodetic antenna anchored in the ice (67.048°N, -
 148 49.018°W, elevation 1211.43 m). On-ice kinematic GPS positions were later estimated using
 149 carrier-phase differential processing relative to a bedrock mounted base station (67.150°N, -
 150 50.058°W, elevation 581.19) and final International GNSS Service satellite orbits (*Chen, 1998;*
 151 *Estey & Meertens, 1999; Hoffman et al., 2011; Andrews et al. 2014; 2018; see SI*). To assess
 152 surface melt processes, simultaneous measurements of 2-m air temperature, energy balance, and
 153 ice ablation were obtained using the nearby PROMICE KAN_M automated weather station
 154 (AWS) (*Fausto and van As, 2019*). To assess proglacial water outflow, hourly discharges were
 155 obtained from permanent river gauges at Qinguata Kuussua (Watson River) in Kangerlussuaq
 156 (*van As et al., 2019*), and its northern tributary Akuliarusiarsuup Kuua near the ice terminus
 157 (*Rennermalm et al., 2017*, AK4 station 67.146°N, 50.107°W). Lagged correlation coefficients
 158 were used to quantify links among these various forcing variables with GPS-derived ice motion.

159 **2.2 Proxies for S and ΔS**

160 GPS-derived vertical positions and their first derivative were used to estimate subglacial
 161 storage S and rate-of-change ΔS (e.g. *Cowton et al., 2016; Bartholomew et al., 2012; see SI*).
 162 Proxies for S and ΔS were also computed by adapting a meltwater input-output approach
 163 (*Bartholomew et al. 2008; 2011; McGrath et al. 2011*) comparing relative timings of supra- and
 164 proglacial discharge hydrographs (see **SI**). Hydrographs were normalized and differenced
 165 (supraglacial minus proglacial) to assess their relative timings and shapes at Rio Behar moulin
 166 and at the ice edge. These “discharge-difference” proxies are unitless and do not satisfy mass
 167 conservation so should be used qualitatively (i.e. for visual comparison of peak S and ΔS timing
 168 with accelerations in ice speed). They also characterize instantaneous net water storage, not
 169 subglacial routing delays and/or storages known to retard proglacial discharges longer than 24 h
 170 (e.g. *Chandler et al., 2013; Chu et al., 2016; Pitcher et al. 2020; Rennermalm et al., 2013b;*
 171 *Smith et al., 2015; van As et al., 2017*). Dye tracing experiments, for example, show that
 172 subglacial routing from ~1300 m elevation takes 1-3 days (*Chandler et al. 2013*, site L57), or ~2-
 173 5 days from proglacial hydrograph analysis (*van As et al., 2017*). Such subglacial delays and
 174 storages are irrelevant to our purpose here, which is simply to characterize instantaneous

175 subglacial conditions at our field site, not Lagrangian transport to the ice edge. Complete
 176 description of these data and methods are presented in SI.
 177



178 **Figure 2:** In situ measurements of (a) melt energy, air temperature, and ice ablation from PROMICE KAN_M; (b)
 179 Rio Behar moulin input (supraglacial river discharge) and proglacial discharge at Kangerlussuaq; (c) Rio Behar ice
 180 surface speed and elevation. Colored envelopes (b, c) represent measurement uncertainties of discharge and ice
 181 motion (see SI).

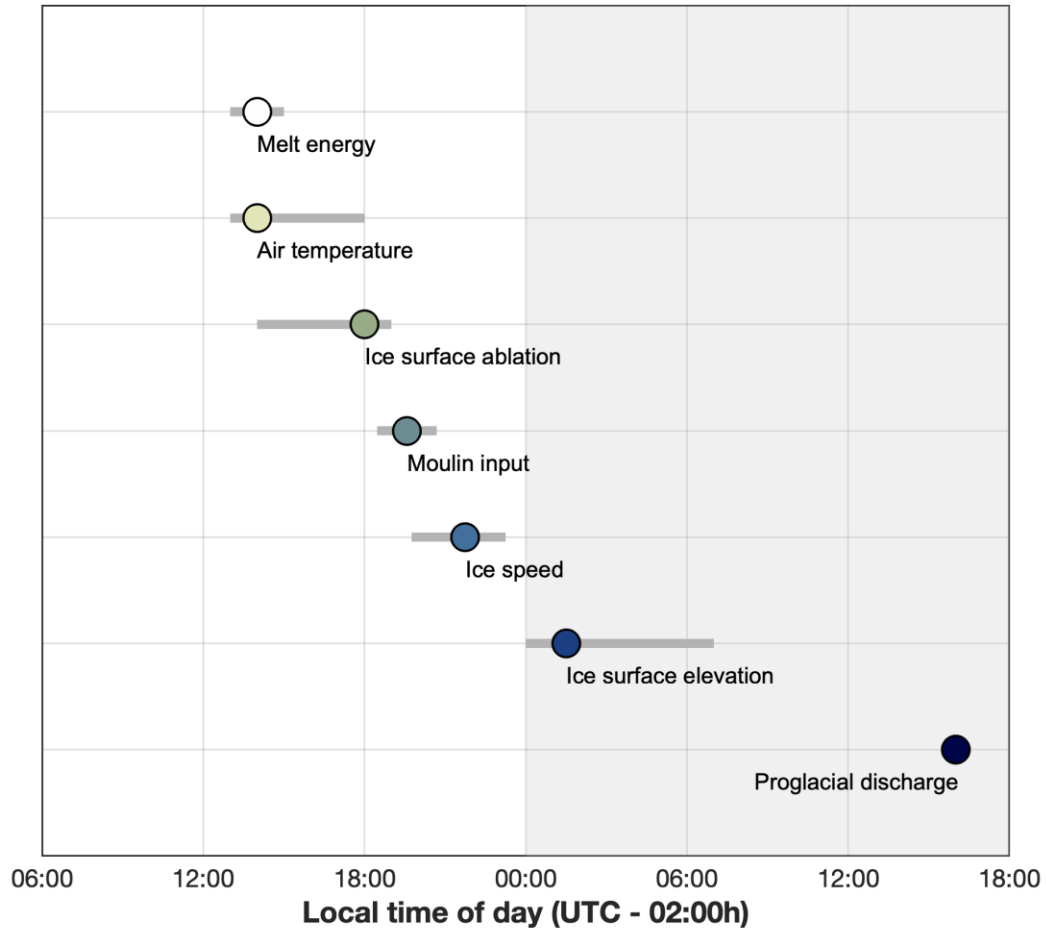
182

183 3. Results

184 3.1 Correlations of ice speed with other variables

185 We find strong diurnal cycles in all variables except surface elevation, with daily
 186 accelerations in horizontal ice speed closely tracking melt energy and moulin input (**Figure 2**).
 187 A consistent progression is observed in the timing of daily peaks, with melt energy and air

188 temperatures peaking near local solar noon, followed by sequential peaks in ice ablation, moulin
 189 input, ice speed, and proglacial discharge (**Figure 3**). The timing of daily peaks is most
 190 consistent for melt energy, moulin input, ice velocity, and proglacial discharge, whereas peaks in



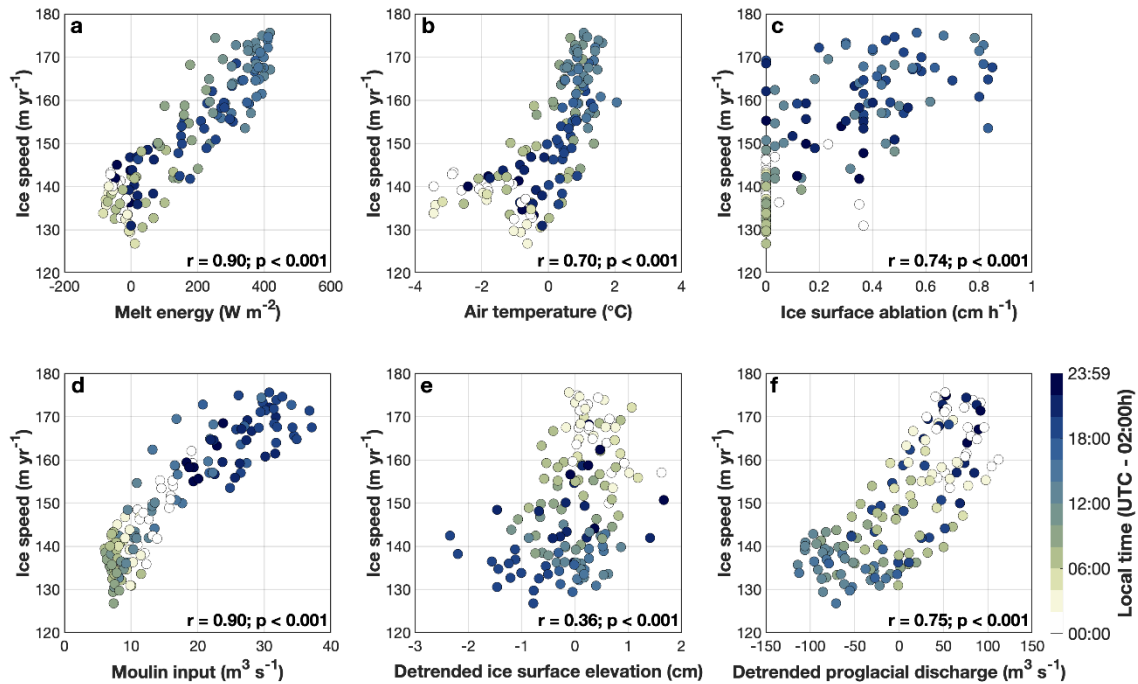
191 air temperature, ablation, and ice surface elevation are more temporally variable (**Figure 3**).

192 **Figure 3: Mean daily timing (circles) and timing range (earliest to latest, grey bars) of daily peaks in observed**
 193 **variables. Diurnal cycles in melt energy and air temperatures peak around solar noon, followed by peaks in ice**
 194 **ablation, moulin meltwater input, ice surface speed, ice surface uplift, and proglacial discharge. Peak proglacial**
 195 **discharge displays no timing variability and is here shifted -8h to account for the mean timing difference**
 196 **between peak daily discharge observed at Kangerlussuaq versus at the ice edge (see SI). Note that this figure**
 197 **presents only the timing of daily peaks, not subglacial routing and/or storages known to delay proglacial**
 198 **discharges longer than 24h.**

199

200 After lagging our GPS-derived horizontal ice speed time-series to correct for mean timing
 201 differences with the other variables, we find ice speed correlates most strongly with melt energy
 202 and moulin input ($r=0.9$, **Figures 4a, 4d**). Moderately strong correlations are found for air
 203 temperature ($r=0.71$, **Figure 4b**) and ice surface ablation rate ($r=0.75$, **Figure 4c**), drivers of melt
 204 energy and runoff, respectively. Lower correlations are found for detrended proglacial discharge
 205 ($r=0.74$, **Figure 2b**) and detrended ice surface elevation (i.e. uplift, $r=0.37$, **Figure 4e**). All

206 correlations are statistically significant ($p < 0.01$). Unlike melt energy (which turns negative,
 207 suggesting nocturnal refreezing), moulin input persists at low levels throughout the night.
 208 Because i) moulin input closely tracks (and derives from) melt energy; ii) virtually all meltwater
 209 runoff generated within Rio Behar catchment flows to its moulin; and iii) the observed +5h
 210 timing difference between peak melt energy and peak supraglacial discharge is similar to a
 211 previously calculated catchment routing delay for Rio Behar (i.e. estimated time-to-peak $t_p = 5.5$ h,
 212 *Smith et al., 2017*) we infer that supraglacial river discharge, a product of catchment-integrated



213 melt energy, is a dominant forcing variable driving our locally recorded ice-speed variations.

214 **Figure 4. Correlations between ice speed and other observed variables, after correcting for the mean differences**
 215 **in daily peak timing shown in Figure 3 (timing differences in parentheses): (a) melt energy (-7h); (b) air**
 216 **temperature (-7h); (c) ablation (-4h); (d) moulin input (-2h); (e) ice surface elevation (+6h); (f) proglacial**
 217 **discharge (+19h at the ice sheet edge). Linear correlations (r) and statistical probability values (p) are shown in**
 218 **the bottom right corner of each plot. Strongest correlations with ice speed are found for melt energy and**
 219 **moulin input.**

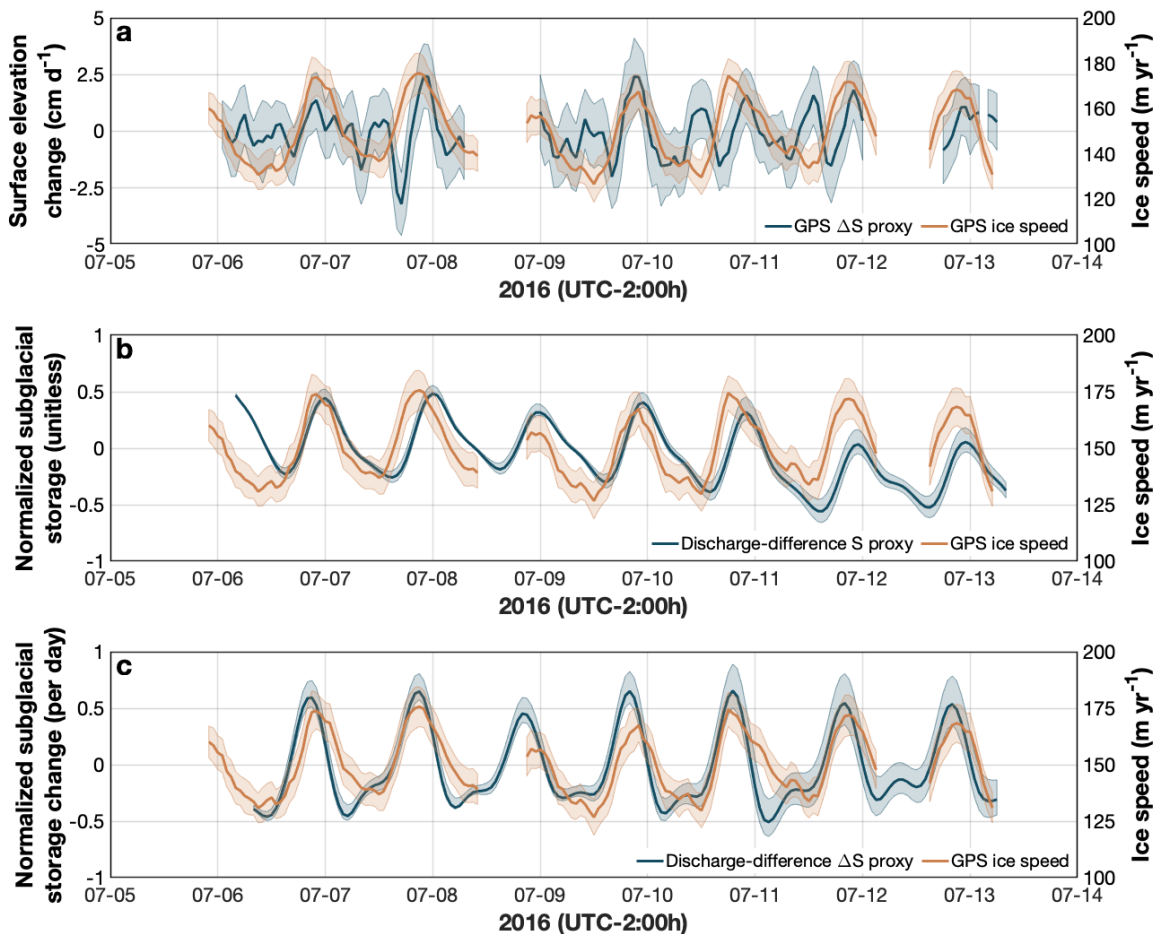
220

221 3.2 Comparison of short-term ice accelerations with S and ΔS

222 To further investigate drivers of ice speed variations, we test proxies of subglacial water
 223 storage S and rate-of-change ΔS calculated from GPS-derived ice surface observations (*Anderson*
 224 *et al., 2004; Andrews et al., 2018; Cowton et al., 2016; Harper et al., 2007; Hoffman et al.,*
 225 *2011; Howat et al., 2008*) and by differencing normalized hydrographs of supraglacial and
 226 proglacial river discharge (See **Methods** and **SI**). Implicit in the latter discharge-difference
 227 calculations are assumptions that englacial storage is negligible; that en/subglacial melting is
 228 negligible; that subglacial routing delays are irrelevant to instantaneous net storage; and that

229 distal (>40 km) proglacial discharge reflects overall regional basal water pressure, allowing Rio
 230 Behar moulin input to be compared with regional proglacial discharge despite its smaller spatial
 231 domain (60 km² vs. ~2800 km² to 1750 m a.s.l.) and absolute discharge magnitude (~6-38 m³ s⁻¹
 232 vs. ~800-1300 m³ s⁻¹).

233 Comparison of our observed horizontal ice speeds with both proxies for S and ΔS
 234 suggests that ΔS drives short-term accelerations in ice speed (**Figure 5b**). This conclusion is
 235 clearest from the discharge-difference proxies, with ΔS aligning better with ice speed peaks and
 236 ascents than S (see **Figure 5c** versus **Figure 5b**, see also **Figure S7**). This same conclusion may
 237 be drawn, albeit less compellingly, from conventional GPS-derived S and ΔS proxies (i.e. **Figure**
 238 **5a** versus **Figure 2c**; **Figure S7**). For both methods, peaks in ΔS generally align better with ice
 239 accelerations than peaks in S , suggesting that changes in subglacial water storage force short-
 240 term ice speed accelerations at our field site.



241 **Figure 5.** Comparison of horizontal ice speeds (blue line) with proxies for subglacial water storage (S) and its
 242 rate-of-change (ΔS): (a) ΔS as estimated from GPS-derived ice surface elevations; (b) S as estimated from
 243 normalized discharge-difference; (c) ΔS as estimated from normalized discharge-difference. See **Figure 2(c)** for S
 244 as estimated from GPS. Short-lived accelerations in ice speed generally align with peaks or ascents in S (c), see
 245 also (a); but not S (b), see also **Figure 2(c)**. Peaks in ΔS capture peaks in ice speed more exclusively in (c) than (a),

246 and also some small secondary ice accelerations, suggesting that the discharge-difference proxy may more
247 sensitively characterize subglacial water storage conditions than vertical GPS measurements.

248 4. Discussion and conclusion

249 We find that diurnal cycles in moulin input (following the integrative and delaying
250 effects of surface routing through the upstream catchment) are the primary driver of short-term
251 accelerations in ice sliding velocity (**Figure 3, Figure 4**). This finding supports previous work
252 (*Andrews et al., 2014*) and the conclusion that over diurnal scales, supraglacial rivers impose a
253 first-order control on subglacial water pressure fluctuations. Furthermore, while short-term
254 accelerations in ice speed closely follow moulin input (**Figure 2, Figure 4**), they also tend to
255 align with proxies for subglacial water storage change (ΔS) better than proxies for absolute
256 storage (S) (**Figure 5, see also Figure 2c**), suggesting that nocturnal peaks in subglacial water
257 storage drive subglacial basal pressure and short-term ice motion.

258 This conclusion is more evident in discharge-difference proxies (**Figures 5b, 5c**) than
259 conventional GPS-derived proxies (**Figures 2c, 5a**). The discharge-discharge ΔS proxy reflects
260 quiescent periods better than GPS-derived ΔS , and may also reflect subglacial behavior
261 associated with a secondary ice-speed peak on most days (**Figure 5c**). Differencing supra- and
262 proglacial hydrographs, therefore, may characterize subglacial water storage conditions more
263 sensitively than small vertical ice surface elevation changes, which are inherently difficult to
264 detect and have multiple sources of uncertainty (*Anderson et al., 2004; 2018*). A meltwater
265 input-output approach (here adapted from *Bartholomew et al., 2008; 2011* and *McGrath et al.,*
266 *2011*), comparing moulin inputs with proglacial outputs, offers an alternate strategy for
267 characterizing subglacial water storage and their link to ice and basal sliding laws. Future
268 studies, for example, could develop discharge-difference proxies over longer time scales and
269 larger study areas by pairing surface-routed climate model output (e.g. *Smith et al., 2017; Yang*
270 *et al., 2019*) with proglacial discharge records (*Rennermalm et al. 2017; van As et al., 2019*), to
271 relate net increases/decreases in ΔS to ice speed variations. Our results, using normalized input
272 and output without mass conservation, suggest that a true (i.e. mass-conserved) water balance
273 may not even be necessary to infer qualitative relationships between subglacial water storage,
274 subglacial pressures, and ice motion.

275 It is well-known that evolution of the subglacial system from inefficient to efficient states
276 acts to modulate the ice dynamical response to supraglacial inputs (e.g. *Bartholomew et al.,*
277 *2010; 2011; Hoffman et al., 2011*). Using two different methods, we find that peak or ascendant
278 ΔS is associated with localized GrIS velocity accelerations (**Figure 5c**). This suggests that
279 highest subglacial water pressures (and ice sliding speeds) occur when subglacial cavities are
280 growing the fastest, not when their size is largest (e.g. *Iken et al., 1983; Cowton et al., 2016*). As
281 such, steady-state theoretical basal sliding laws – which assume a relationship between cavity
282 size and subglacial pressure – do not accurately represent transient behavior of the subglacial
283 system.

284 It is important to note that the strong correlation between moulin input and ice velocity
285 reported here (**Figure 4d**) is unlikely to hold over an entire melt season. Previous work has
286 clearly established that Greenland ice sliding velocities are strongly influenced by long-term
287 seasonal evolution of the subglacial hydrological system (*Hoffman et al., 2011; Andrews et al.,*
288 *2018; Bartholomew et al., 2010; Nienow et al., 2017*). Our short 7-day record captures neither

289 the early nor late melt season, when subglacial efficiency (and associated ice speeds) undergo
290 extensive changes. Subglacial evolution makes melt-driven proxies inappropriate for estimating
291 ice motion over the entire melt season (*Andrews et al., 2014, Bartholomew et al., 2010*) or
292 multiple years (*Tedstone et al., 2015; Davison et al., 2019*). Over short time scales, however, we
293 find that diurnal cycles in moulin input are the primary driver of fluctuating subglacial water
294 pressures and associated ice accelerations – even in relatively thick ice (~1 km) more than 40 km
295 inland from the ice edge. Some slight variability in peak timings between ΔS and ice motion, as
296 well as non-linear behavior on descending limbs (**Figure 5c**) are discussed further in **SI (Text**
297 **S8)**

298 This study adds to a small but growing collection of GrIS supraglacial streamflow
299 measurements (*Holmes 1955; Echelmeyer and Harrison 1990; Carver et al. 1994; McGrath et*
300 *al. 2011; Chandler et al., 2013; Gleason et al. 2016; Smith et al., 2015; 2017*). With peak daily
301 discharges of 26.59 – 37.61 m³/s (**Table S2**), the discharges reported here are far larger than
302 those collected in most supraglacial streams, but are typical for trunk supraglacial rivers in
303 southwest Greenland (*Smith et al., 2015; 2017*). Nearly all of them terminate in moulins (*Smith*
304 *et al., 2015; Yang and Smith, 2016*), and the high diurnal variability we observe (19.05 – 30.50
305 m³/s, **Table S2**) signifies that local subglacial channels are likely out of equilibrium with moulin
306 input for large portions of the day, such that corresponding accelerations in ice speed are driven
307 by addition or removal of water outside of the channelized system.

308 Based on satellite mapping (e.g. *Yang and Smith, 2013; 2016; Lampkin and VanderBerg,*
309 *2014; Smith et al., 2015; Yang et al., 2015; 2016*) and topographic modeling (e.g. *Banwell et al.*
310 *2012; 2016; King et al., 2016; Karlstrom and Yang, 2016; Crozier et al., 2018*), we submit that
311 supraglacial rivers likely drive ice accelerations near hundreds of other terminal moulins as well.
312 Process-level understanding and modeling of subglacial hydrology and associated ice dynamics
313 should presume large, strongly diurnal inputs of meltwater entering hundreds of supraglacial
314 river moulins distributed throughout Greenland’s ablation zone. These inputs, countered by
315 water output discharged beneath outlet glaciers, trigger short-term fluctuations in subglacial
316 water storage that drive short-term accelerations in ice sheet motion.

317

318 **5. Data Availability**

319 Supraglacial discharges, surface mass balance variables, ADCP and GPS data, and S and
320 ΔS proxies are provided as summary tables (**Tables S1-S2**) and/or as Additional Supporting
321 Information (**Datasets S1-S7**). PROMICE KAN_M automated weather station data (*Fausto and*
322 *van As, 2019*) are available from <https://www.promice.org/PromiceDataPortal/>. Proglacial river
323 discharges for Qinguata Kuussua/Watson River (*van As et al., 2019*) and Akuliarusiarsuup
324 Kuua (*Rennermalm et al., 2013b; 2017*) are available from
325 https://doi.org/10.22008/promice/data/watson_river_discharge and
326 <https://doi.org/10.1594/PANGAEA.876357>.

327

328 **6. Acknowledgements**

329 This research was funded by the NASA Cryospheric Science Program (grants
330 80NSSC19K0942 and NNX14AH93G) managed by Dr. Thorsten Markus. Polar Field Services,
331 Inc. and Kangerlussuaq International Science Support (KISS) provided logistical field support.
332 GPS equipment was loaned by UNAVCO, Inc. with support from NASA and NSF. A. Zaino and
333 J. Pettit of UNAVCO advised on GPS receiver hardware, programming, and installation.
334 Proglacial discharge data from Qinguata Kuussua/Watson River were gathered by the
335 University of Copenhagen and the Geological Survey of Denmark and Greenland. The KAN_M
336 weather station is part of the Programme for Monitoring of the Greenland Ice Sheet
337 (www.PROMICE.dk). The authors declare there are no real or perceived financial conflicts of
338 interest, or other affiliations for any author that may be perceived as having a conflict of interest
339 with respect to the results of this research.

340

341 **Dedication**

342 We dedicate this paper to the memory of Konrad Steffen (1952-2020).

343

344 **References**

345

346 Andrews L.C., Catania G.A., Hoffman M.J., Gullett J.D., Lüthi M.P., et al. (2014), Direct
347 observations of evolving subglacial drainage beneath the Greenland Ice Sheet. *Nature*, 514,
348 80–83, <https://doi.org/10.1038/nature13796>

349 Andrews, L.C., Hoffman, M.J., Neumann, T.A., Catania, G.A., Lüthi, M.P., Hawley, R.L., et al.
350 (2018), Seasonal evolution of the subglacial hydrologic system modified by supraglacial
351 lake drainage in western Greenland. *Journal of Geophysical Research-Earth Surface*, 123,
352 1479–1496. <https://doi.org/10.1029/>

353 Anderson, R.S., Anderson, S.P., MacGregor, K.R., Waddington, E.D., O’Neel, S., Riihimäki,
354 C.A., Loso, M.G. (2004), Strong feedbacks between hydrology and sliding of a small
355 alpine glacier. *Journal of Geophysical Research—Earth Surface*, 109(F3), F03005.
356 <https://doi.org/10.1029/2004JF000120>

357 Banwell, A.F., Arnold, N.S., Willis, I.C., Tedesco, M., Ahlstrom, A.P. (2012), Modelling
358 supraglacial water routing and lake filling on the Greenland ice sheet. *J. Geophys. Res.*,
359 117, F04012, doi:10.1029/2012JF002393.

360 Banwell, A., Hewitt, I., Willis, I., Arnold, N. (2016), Moulin density controls drainage
361 development beneath the Greenland ice sheet. *J. Geophys. Res. Earth Surf.*, 121, 2248–
362 2269, doi:10.1002/2015JF003801.

363 Bartholomäus, T.C., Anderson, R.S., Anderson, S.P. (2008), Response of glacier basal motion to
364 transient water storage. *Nature Geoscience*, 1, 33–37. <https://doi.org/10.1038/ngeo.2007.52>

365 Bartholomäus, T.C., Anderson, R.S., Anderson, S.P. (2011), Growth and collapse of the
366 distributed subglacial hydrologic system of Kennicott Glacier, Alaska, USA, and its effects

- 367 on basal motion. *Journal of Glaciology*, 57(206), 985-1002, DOI:
368 <https://doi.org/10.3189/002214311798843269>
- 369 Bartholomew, I., Nienow, P., Mair, D. et al. (2010), Seasonal evolution of subglacial drainage
370 and acceleration in a Greenland outlet glacier. *Nature Geosci.*, 3, 408–411,
371 <https://doi.org/10.1038/ngeo863>
- 372 Bartholomew, I., Nienow, P., Sole, A., Mair, D., Cowton, T., Palmer, S., Wadham, J. (2011),
373 Supraglacial forcing of subglacial drainage in the ablation zone of the Greenland ice sheet.
374 *Geophys. Res. Lett.*, 38, L08502, doi:10.1029/2011GL047063.
- 375 Bartholomew, I. D., Nienow, P., Sole, A., Mair, D., Cowton, T., King, M. A. (2012), Short-term
376 variability in Greenland Ice Sheet motion forced by time-varying meltwater drainage:
377 Implications for the relationship between subglacial drainage system behavior and ice
378 velocity. *Journal of Geophysical Research: Earth Surface*, 117(F3), F03002.
379 <https://doi.org/10.1029/2011JF002220>
- 380 Bell, R. (2008) The role of subglacial water in ice-sheet mass balance. *Nature Geosci*, 1, 297–
381 304, <https://doi.org/10.1038/ngeo186>
- 382 Bindschadler, R. (1983), The importance of pressurized subglacial water in separation and
383 sliding at the glacier bed. *Journal of Glaciology*, 29(101), 3–19.
384 <https://doi.org/10.3189/S0022143000005104>
- 385 Carver S., Sear D., Valentine E. (1994) An observation of roll waves in a supraglacial meltwater
386 channel, Harlech Gletscher, East Greenland. *J. Glaciology* 40(134):75–78
- 387 Catania G.A., Neumann T.A. (2010), Persistent englacial drainage features in the Greenland Ice
388 Sheet. *Geophys. Res. Lett.*, 37:1–5, <https://doi.org/10.1029/2009GL041108>
- 389 Chandler, D. M., Wadham, J. L., Lis, G. P., Cowton, T., Sole, A., Bartholomew, I., ... Hubbard,
390 A. (2013), Evolution of the subglacial drainage system beneath the Greenland Ice Sheet
391 revealed by tracers. *Nature Geoscience*, 6(3), 195–198. <https://doi.org/10.1038/ngeo1737>
392
- 393 Chen, G. (1998). GPS kinematic positioning for airborne laser altimetry at Long Valley,
394 California. Massachusetts Institute of Technology, Cambridge, MA. Retrieved from
395 <http://dspace.mit.edu/handle/1721.1/9680>
- 396 Chu, V. W. (2014), Greenland ice sheet hydrology: a review, *Prog. Phys. Geogr.*, 38(1), 19-54.
- 397 Chu W., Schroeder D.M., Seroussi H., Creyts T.T., Palmer S.J., Bell R.E. (2016), Extensive
398 winter subglacial water storage beneath the Greenland Ice Sheet. *Geophys. Res. Lett.*
399 43(24):12,484-12,492
- 400 Clason C.C., Mair D.W.F., Nienow P.W., Bartholomew I.D., Sole A., et al. (2015), Modelling
401 the transfer of supraglacial meltwater to the bed of Leverett Glacier, Southwest Greenland.
402 *The Cryosphere*, 9(1), 123–38. [www.the-cryosphere.net/9/123/2015/doi:10.5194/tc-9-123-](http://www.the-cryosphere.net/9/123/2015/doi:10.5194/tc-9-123-2015)
403 2015
- 404 Cooper M.G., Smith L.C., Rennermalm A.K., Miège C., Pitcher L.H, et al. (2018), Meltwater
405 storage in low-density near-surface bare ice in the Greenland ice sheet ablation zone. *The*
406 *Cryosphere* 12(3):955–70

- 407 Cooper, M.G., Smith, L.C. (2019) Satellite Remote Sensing of the Greenland Ice Sheet Ablation
408 Zone: A Review. *Remote Sensing*, 11, 2405. DOI: 10.3390/rs11202405
- 409 Cowton T., Nienow P., Sole A., Wadham J., Lis G., et al. (2013), Evolution of drainage system
410 morphology at a land-terminating Greenlandic outlet glacier. *J. Geophys. Res. Earth Surf.*
411 118(1):29–41
- 412 Cowton, T., Nienow, P., Sole, A., Bartholomew, I., Mair, D. (2016), Variability in ice motion at
413 a land-terminating Greenlandic outlet glacier: the role of channelized and distributed
414 drainage systems. *Journal of Glaciology*, doi:10.1017/jog.2016.36
- 415 Crozier, J., Karlstrom, L., and Yang, K. (2018), Basal control of supraglacial meltwater
416 catchments on the Greenland Ice Sheet, *The Cryosphere*, 12, 3383–3407,
417 <https://doi.org/10.5194/tc-12-3383-2018>
- 418 Davison, B.J., Sole, A.J., Livingstone, S.J., Cowton, T.R., Nienow, P.W. (2019) The influence of
419 hydrology on the dynamics of land-terminating sectors of the Greenland ice sheet.
420 *Frontiers in Earth Science*, 7(10), ISSN 2296-6463
421 <https://doi.org/10.3389/feart.2019.00010>
- 422 Echelmeyer K., Harrison W.D. (1990) Jakobshavns Isbræ, West Greenland: seasonal variations
423 in velocity—or lack thereof. *J. Glaciology*, 36(122):82–88.
424
- 425 Estey, L.H., and Meertens, C.M. (1999) TEQC: The Multi-Purpose Toolkit for GPS/GLONASS
426 Data. *GPS Solutions* (pub. by John Wiley & Sons), Vol. 3(1), 42-49,
427 <https://doi.org/10.1007/PL00012778>
- 428 Fausto, R.S. and van As, D., (2019). Programme for monitoring of the Greenland ice sheet
429 (PROMICE): Automatic weather station data. Version: v03, Dataset published via
430 Geological Survey of Denmark and Greenland. DOI:
431 <https://doi.org/10.22008/promice/data/aws>
- 432 Flowers, G., Jarosch, A., Belliveau, P., Fuhrman, L. (2016), Short-term velocity variations and
433 sliding sensitivity of a slowly surging glacier. *Annals of Glaciology*, 57(72), 71-83.
434 doi:10.1017/aog.2016.7
- 435 Flowers, G.E. (2018), Hydrology and the future of the Greenland Ice Sheet. *Nature*
436 *Communications*, 9(2729). DOI: 10.1038/s41467-018-05002-0
- 437 Gagliardini, O., Cohen, D., Råback, P. Zwinger, T. (2007) Finite-element modeling of subglacial
438 cavities and related friction law. *J. Geophys. Res.* 112, F02027.
- 439 Gleason, C.J., Smith, L.C., Chu, V.W., Legleiter, C.J., Pitcher, L.H., Overstreet, B.T.,
440 Rennermalm, A.K., Forster, R.R., and Yang, K. (2016), Characterizing supraglacial
441 meltwater channel hydraulics on the Greenland Ice Sheet from in situ observations. *Earth*
442 *Surf. Process. Landforms*, 41: 2111– 2122. doi: 10.1002/esp.3977.
- 443 Harper, J. T., Humphrey, N. F., Pfeffer, W. T., Lazar, B. (2007), Two modes of accelerated
444 glacier sliding related to water. *Geophysical Research Letters*, 34(12), L12503.
445 <https://doi.org/10.1029/2007GL030233>

- 446 Hoffman M.J., Catania G.A., Neumann T.A., Andrews L.C., Rumrill J.A. (2011), Links between
447 acceleration, melting, and supraglacial lake drainage of the western Greenland Ice Sheet. *J.*
448 *Geophys. Res.*, 116, F04035
- 449 Hoffman, M., Andrews, L., Price, S. et al. (2016), Greenland subglacial drainage evolution
450 regulated by weakly connected regions of the bed. *Nature Communications*, 7, 13903.
451 <https://doi.org/10.1038/ncomms13903>
- 452 Holmes G. 1955. Morphology and hydrology of the Mint Julep area, southwest Greenland. In
453 Project Mint Julep: Investigation of Smooth Ice Areas of the Greenland Ice Cap, 1953; Part
454 II: Special Scientific Reports. Maxwell Air Force Base, AL: Arct. Desert Tropic Inf. Cent.,
455 Res. Stud. Inst., Air Univ.
- 456 Howat, I.M., Tulaczyk, S., Waddington, E., Björnsson, H. (2008), Dynamic controls on glacier
457 basal motion inferred from surface ice motion. *Journal of Geophysical Research: Earth*
458 *Surface*, 113(F3), F03015. <https://doi.org/10.1029/2007JF000925>
- 459 Iken, A. Röthlisberger, H., Flotron, A., W. Haeberli, W. (1983) The uplift of Unteraargletscher at
460 the beginning of the melt season — a consequence of water storage at the bed? *J. Glaciol.*,
461 29(101), 28–47
- 462 Irvine-Fynn, T.D.L., A.J. Hodson, B.J. Moorman, G. Vatne, A.L. Hubbard (2011), Polythermal
463 glacier hydrology: a review, *Rev. Geophys.*, 49(4), RG4002.
- 464 Jansson, P. (1996), Dynamics and hydrology of a small polythermal valley glacier. *Geografiska*
465 *Annaler: Series A, Physical Geography*, 78, 171–180.
- 466 Kamb, B. (1970), Sliding motion of glaciers: Theory and observation. *Reviews of Geophysics*,
467 8(4), 673–728. <https://doi.org/10.1029/RG008i004p00673>
- 468 Karlstrom, L., Yang, K. (2016), Fluvial supraglacial landscape evolution on the Greenland Ice
469 Sheet, *Geophys. Res. Lett.*, 43, 2683–2692, doi:10.1002/2016GL067697.
- 470 King L., Hassan M.A., Yang K., Flowers G. (2016), Flow Routing for Delineating Supraglacial
471 Meltwater Channel Networks. *Remote Sensing*, 8(12):988. doi:10.3390/rs8120988
- 472 Lampkin, D.J., VanderBerg, J. (2014), Supraglacial melt channel networks in the Jakobshavn
473 Isbræ region during the 2007 melt season, *Hydrol. Process.*, 28, 6038–6053, doi:
474 10.1002/hyp.10085
- 475 Lindbäck, K., Pettersson, R., Hubbard, A.L., Doyle, S.H., van As, D., Mikkelsen, A.B.,
476 Fitzpatrick, A.A. (2015). Subglacial water drainage, storage, and piracy beneath the
477 Greenland Ice Sheet. *Geophysical Research Letters*, 42(18), 7606–7614.
478 <https://doi.org/10.1002/2015GL065393>
- 479 Mair, D., Sharp, M.J., Willis, I.C. (2002), Evidence for basal cavity opening from analysis of
480 surface uplift during a high-velocity event: Haut Glacier d’Arolla, Switzerland. *Journal of*
481 *Glaciology*, 48(161), 208–216. <https://doi.org/10.3189/172756502781831502>
- 482 McGrath D., Colgan W., Steffen K., Lauffenburger P., Balog J. (2011), Assessing the summer
483 water budget of a moulin basin in the Sermeq Avannarleq ablation region, Greenland ice
484 sheet. *J. Glaciol.* 57(205):954–64

- 485 Meierbachtol, T., J. Harper, N. Humphrey (2013), Basal Drainage System Response to
486 Increasing Surface Melt on the Greenland Ice Sheet. *Science*, 341, 6147, 777-779. DOI:
487 10.1126/science.1235905
- 488 Morlighem, M., Williams, C. N., Rignot, E., An, L., Arndt, J. E., Bamber, J. L., ... Zinglensen,
489 K. B. (2017), BedMachine v3: Complete bed topography and ocean bathymetry mapping of
490 Greenland from multibeam echo sounding combined with mass conservation, *Geophysical
491 Research Letters*, 44, 11,051– 11,061. <https://doi.org/10.1002/2017GL074954> [Data
492 accessed 7/20 at Morlighem, M. et al. 2017, updated 2018. IceBridge BedMachine
493 Greenland, Version 3. Boulder, Colorado USA. NASA National Snow and Ice Data Center
494 Distributed Active Archive Center. doi: <https://doi.org/10.5067/2CIX82HUV88Y>]
- 495 Nienow, P.W., Sole, A.J., Slater, D.A., Cowton, T.R. (2017), Recent Advances in Our
496 Understanding of the Role of Meltwater in the Greenland Ice Sheet System. *Curr Clim
497 Change Rep* (2017) 3:330–344, DOI 10.1007/s40641-017-0083-9
- 498 Palmer S., Shepherd A., Nienow P., Joughin I. (2011), Seasonal speedup of the Greenland ice
499 sheet linked to routing of surface water. *Earth Planet. Sci. Lett.* 302(3–4):423–28
- 500 Pitcher, L.H., Smith, L.C. (2019), Supraglacial Streams and Rivers. *Annual Review of Earth and
501 Planetary Sciences*, 47(1), 421-452, <https://doi.org/10.1146/annurev-earth-053018-060212>
- 502 Pitcher, L.H., Smith, L.C., Gleason, C.J., Miede, C., Ryan, J.C., Hagedorn, B., van As, D., Chu,
503 W., Forster, R.R. (2020) Direct observation of wintertime meltwater drainage from the
504 Greenland Ice Sheet. *Geophysical Research Letters*, e2019GL086521,
505 <https://doi.org/10.1029/2019GL086521>
- 506 Rennermalm, Å.K., Moustafa, S.E., Mioduszewski, J., Chu, V.W., Forster, R.R., Hagedorn, B.,
507 Harper, J.T., Mote, T.L., Robinson, D.A., Shuman, C.A., et al. (2013a), Understanding
508 Greenland ice sheet hydrology using an integrated multi-scale approach. *Environ. Res. Lett.*
509 2013, 8, 015017.
- 510 Rennermalm, Å.K., Smith, L. C., Chue, V.W., Box, J.E., Forster, R.R., Van den Broeke, M. R.
511 (2013b), Evidence of meltwater retention within the Greenland ice sheet. *The Cryosphere*,
512 7, 1433–1445, 2013. <https://doi.org/10.5194/tc-7-1433-2013>
- 513 Rennermalm, A.K., Smith, L.C., Hammann, A.C., Leidman, S.Z., Cooper, M.G., Cooley, S.W.,
514 Pitcher, L. (2017), River discharge at station AK-004-001, 2008 - 2016, version 3.0. The
515 State University of New Jersey, PANGAEA, <https://doi.org/10.1594/PANGAEA.876357>
- 516 Ryan, J.C., Smith, L.C., van As, D., Cooley, S.W., Cooper, M.G., Pitcher, L.H, Hubbard, A.
517 (2019), Greenland Ice Sheet surface melt amplified by snowline migration and bare ice
518 exposure *Science Advances* 5(3), eaav3738, DOI: 10.1126/sciadv.aav3738
- 519 Schoof, C. (2010), Ice-sheet acceleration driven by melt supply variability. *Nature*.
520 468(7325):803
- 521 Schoof, C. (2005), The effect of cavitation on glacier sliding. *Proc. R. Soc. A.* 461609–627
522 <http://doi.org/10.1098/rspa.2004.1350>.
- 523 Schweizer, J., Iken, A. (1992), The role of bed separation and friction in sliding over an
524 undeformable bed. *Journal of Glaciology*, 38(128), 77–92.
525 <https://doi.org/10.3189/S0022143000009618>

- 526 Sugiyama, S., Gudmundsson, H. (2004), Short-term variations in glacier flow controlled by
527 subglacial water pressure at Lauteraargletscher, Bernese Alps, Switzerland. *Journal of*
528 *Glaciology*, 50(170), 353–362. <https://doi.org/10.3189/172756504781829846>
- 529 Shepherd, A., Hubbard, A., Nienow, P., King, M., McMillan, M., Joughin, I. (2009), Greenland
530 ice sheet motion coupled with daily melting in late summer, *Geophys. Res. Lett.*, 36,
531 L01501, doi:10.1029/2008GL035758.
- 532 Smith, L.C., Chu, V.W., Yang, K., Gleason, C.J., Pitcher, L.H., Rennermalm, Å.K., et al. (2015),
533 Efficient meltwater drainage through supraglacial streams and rivers on the southwest
534 Greenland Ice Sheet. *Proceedings of the National Academy of Sciences*, 112 (4) 1001-1006.
535 <https://doi.org/10.1073/pnas.1413024112>
- 536 Smith, L.C., Yang, K., Pitcher, L.H., Overstreet, B.T., Chu, V.W., Rennermalm, Å.K., et al.
537 (2017), Direct measurements of meltwater runoff on the Greenland Ice Sheet surface.
538 *Proceedings of the National Academy of Sciences*, 114(50), E10622-E10631, DOI:
539 10.1073/pnas.1707743114
- 540 Tedstone, A.J., Nienow, P.W., Sole, A.J., Mair, D.W.F., Cowton, T.R., Bartholomew, I.D., King,
541 M.A. (2013) Greenland ice sheet motion insensitive to exceptional meltwater forcing.
542 *Proceedings of the National Academy of Sciences*, 110 (49) 19719-19724; DOI:
543 10.1073/pnas.1315843110
- 544 Tedstone, A., Nienow, P., Gourmelen, N., Dehecq, A., Goldberg, D., Hanna, E. (2015), Decadal
545 slowdown of a land-terminating sector of the Greenland Ice Sheet despite warming.
546 *Nature*, 526, 692–695. <https://doi.org/10.1038/nature15722>
- 547 van As, D., Bech Mikkelsen, A., Holtegaard Nielsen, M., Box, J. E., Claesson Liljedahl, L.,
548 Lindbäck, K., Pitcher, L., Hasholt, B. (2017), Hypsometric amplification and routing
549 moderation of Greenland ice sheet meltwater release. *The Cryosphere*, 11, 1371–1386,
550 <https://doi.org/10.5194/tc-11-1371-2017>
- 551 van As, D., Bent Hasholt, Andreas P. Ahlstrøm, Jason E. Box, John Cappelen, William Colgan,
552 Robert S. Fausto, Sebastian H. Mernild, Andreas Bech Mikkelsen, Brice P.Y. Noël, Dorthe
553 Petersen, Michiel R. van den Broeke (2018) Reconstructing Greenland Ice Sheet meltwater
554 discharge through the Watson River (1949–2017), *Arctic, Antarctic, and Alpine Research*,
555 50:1, DOI: 10.1080/15230430.2018.1433799
- 556 van As, D., Hasholt, B., Ahlstrøm, A.P., Box, J.E., Cappelen, J., Colgan, W., Fausto, R.S.,
557 Mernild, S.H., Mikkelsen, A.B., Noël, B.P.Y., Petersen, D., van den Broeke, M.R. (2018),
558 Reconstructing Greenland Ice Sheet meltwater discharge through the Watson River (1949–
559 2017), *Arctic, Antarctic, and Alpine Research*, 50:1, DOI:
560 10.1080/15230430.2018.1433799
- 561 van As, D., Hasholt, B., Ahlstrøm, A. P., Box, J. E., Cappelen, J., Colgan, W., Fausto, R.S.,
562 Mernild, S.H., Mikkelsen, A.P., Noël, B.P.Y., Petersen, D., van den Broeke, M. R. (2019).
563 Programme for monitoring of the Greenland ice sheet (PROMICE): Watson river
564 discharge. Version: v01, Dataset published via Geological Survey of Denmark and
565 Greenland. https://doi.org/10.22008/promice/data/watson_river_discharge

- 566 van de Wal, R. S. W., W. Boot, M. R. Van den Broeke, C. J. P. P. Smeets, C. H. Reijmer, J. J. A.
567 Donker, J. Oerlemans (2008), Large and rapid melt-induced velocity changes in the
568 ablation zone of the Greenland ice sheet, *Science*, 321(5885), 111-113.
- 569 van de Wal, R.S.W., Smeets, C.J.P.P., Boot, W., Stoffelen, M., van Kampen, R., Doyle, S.H.,
570 Wilhelms, F., van den Broeke, M.R., Reijmer, C.H., Oerlemans, J., Hubbard, A. (2015),
571 Self-regulation of ice flow varies across the ablation area in south-west Greenland, *The*
572 *Cryosphere*, 9, 603–611, <https://doi.org/10.5194/tc-9-603-2015>
- 573 Williams, J.J., Gourmelen, N., Nienow, P. (2020), Dynamic response of the Greenland ice sheet
574 to recent cooling. *Sci Rep*, 10, 1647. <https://doi.org/10.1038/s41598-020-58355-2>
- 575 Yang, K., Smith, L.C., Supraglacial Streams on the Greenland Ice Sheet Delineated From
576 Combined Spectral-Shape Information in High-Resolution Satellite Imagery. *IEEE*
577 *Geoscience and Remote Sensing Letters*, 10(4), 801–805,
578 doi:10.1109/LGRS.2012.2224316, 2013
- 579 K. Yang, Smith, L.C., Chu, V.W., Gleason, C.J., Li, M. (2015), A Caution on the Use of Surface
580 Digital Elevation Models to Simulate Supraglacial Hydrology of the Greenland Ice Sheet.
581 *IEEE Journal of Selected Topics in Applied Earth Observations and Remote Sensing*,
582 8(11), 5212-5224, doi: 10.1109/JSTARS.2015.2483483.
- 583 Yang K., Smith L.C. (2016), Internally drained catchments dominate supraglacial hydrology of
584 the southwest Greenland Ice Sheet. *J. Geophys. Res. Earth Surf.*, 1891–1910.
585 doi:10.1002/2016JF003927
- 586 Yang, K., Smith, L.C., Karlstrom, L., Cooper, M.G., Tedesco, M., van As, D., Cheng, X., Chen,
587 Z., Li, M.(2018), A new surface meltwater routing model for use on the Greenland Ice
588 Sheet surface, *The Cryosphere*, 12, 3791–3811, <https://doi.org/10.5194/tc-12-3791-2018>
- 589 Yang, K., Smith, L.C., Fettweis, X., Gleason, C.J., Lu, Y., Li, M. (2019) Surface meltwater
590 runoff on the Greenland ice sheet estimated from remotely sensed supraglacial lake
591 infilling rate (2019). *Remote Sensing of Environment*, 234, 111459,
592 <https://doi.org/10.1016/j.rse.2019.111459>
- 593 Yang, K., Sommers, A., Andrews, L.C., Smith, L. C., Lu, X., Fettweis, X., Li, M. (2020) Inter-
594 comparison of surface meltwater routing models for the Greenland Ice Sheet and influence
595 on subglacial effective pressures, *The Cryosphere Discuss.*, [https://doi.org/10.5194/tc-](https://doi.org/10.5194/tc-2019-255)
596 2019-255.
- 597 Zwally, H.J., Abdalati, W., Herring, T., Larson, K., Saba, J., Steffen, K. (2002), Surface melt
598 induced acceleration of Greenland ice-sheet flow, *Science*, 297(5579), 218-222.